Published in final edited form as:
Immunity. 2010 July 23; 33(1): 48–59. doi:10.1016/j.immuni.2010.06.013.

MicroRNA-34a perturbs B lymphocyte development by repressing the Forkhead Box Transcription Factor Foxp1

Dinesh S. Rao[1,2,3], **Ryan M. O'Connell**[1], **Aadel A. Chaudhuri**[1], **Yvette Garcia-Flores**[1], **Theresa L. Geiger**[1], and **David Baltimore**[1]

[1] Division of Biology, California Institute of Technology, Pasadena, CA

[2] Department of Pathology and Laboratory Medicine , UCLA-David Geffen School of Medicine, Los Angeles, CA

[3] Jonnson Comprehensive Cancer Center, UCLA-David Geffen School of Medicine, Los Angeles, CA

Summary

MicroRNAs (miRNAs) can influence lineage choice or affect critical developmental checkpoints during hematopoiesis. To search for a role of the recently described p53-induced microRNA, miR-34a, in hematopoiesis, we performed gain-of-function analysis in murine bone marrow. Constitutive expression of miR-34a led to a block in B cell development at the pro-B cell to pre-B cell transition, leading to a reduction in mature B cells. This block appeared to be mediated primarily by inhibited expression of the Forkhead transcription factor, Foxp1. We demonstrated that Foxp1 was a direct target of miR-34a in a 3′-untranslated region (UTR)-dependent fashion. Knockdown of *Foxp1* by siRNA recapitulated the B cell developmental phenotype induced by miR-34a, whereas co-transduction of *Foxp1* lacking its 3′UTR with miR-34a rescued B cell maturation. Lastly, knockdown of miR-34a resulted in increased amounts of Foxp1 and mature B cells. These findings identify a role for miR-34a in connecting the p53 network with suppression of Foxp1, a known B cell oncogene.

Introduction

Antigen-independent B cell development from hematopoietic stem and progenitor cells is a complex process, closely coordinated with the generation of functional antigen receptors (Hardy and Hayakawa, 2001). B cells are the end product of an ordered series of developmental steps punctuated by checkpoints following the rearrangement of the immunoglobulin heavy (IgH) and light chain (IgL) loci. Defined stages of committed B cell precursors include pro-B cells, during which B cells rearrange IgH, pre-B cells, during which IgL is rearranged, and finally immature and mature B cells expressing variable amounts of surface immunoglobulin (IgM). A complex sequence of molecular events orchestrates successful V(D)J rearrangement in B cells. It includes the activation of several transcription factors, notably PU.1, E2a, Ebf, and Pax5 (Busslinger, 2004). A recent addition to the list of transcription factors required for early B cell development is Foxp1 (Hu et al., 2006). By using a recombination activating gene-2 (*Rag2*) complementation system, loss of

Corresponding author: Dr. David Baltimore, Division of Biology, California Institute of Technology, 1200 E. California Blvd, M/C 147-75, Pasadena, CA 91125., baltimo@caltech.edu.

this transcription factor was found to cause a block in early B cell development. Furthermore, a functional role in coordinating the development of B cells was suggested by Foxp1's ability to bind to enhancer elements within the *Rag* gene loci (Hu et al., 2006). Foxp1 is a forkhead transcription factor with functions in tissue and cell-type specific gene expression and its targeted deletion is lethal in embryogenesis, mainly due to cardiac defects (Shu et al., 2001; Wang et al., 2004).

During B cell development, multiple checkpoints follow the rearrangement of the immunoglobulin loci (Meffre et al., 2000) that are partially dependent on p53 (encoded by *Trp53*). *Trp53*$^{-/-}$ mice show decreased apoptosis of pro-B cells, as well as accumulation of pre-B cells and immature B cells (Alizadeh et al., 2000; Lu and Osmond, 2000). Additionally, in SCID mice, deficiency of *Trp53* leads to a massive accumulation of pro-B cells (Guidos et al., 1996). Presumably, such cells would normally undergo apoptosis as consequence of p53's action in coordinating the response of cells to DNA damage. The apoptosis of pro-B cells depends on the ratio of pro-apoptotic Bax to the pro-survival Bcl-2 protein, and this ratio is disrupted in *Trp53*$^{-/-}$ mice.

Recently, the miR-34 family of miRNAs was discovered to be transcriptionally induced by p53 (Chang et al., 2007; He et al., 2007; Raver-Shapira et al., 2007). These miRNAs act by suppressing genes important in cell cycle progression, anti-apoptotic functions, and regulation of cell growth. As might be expected, expression of these miRNAs is altered in a broad range of cancers, with the most common scenario being one in which both p53 and miR-34 are downregulated (reviewed in (Hermeking, 2009)). In cancers of the hematopoietic system, profiling studies have suggested a role for one member of the miR-34 family, miR-34a, in chronic lymphocytic leukemia and acute myeloid leukemia (Isken et al., 2008; Mraz et al., 2009; Zenz et al., 2009). In the case of chronic lymphocytic leukemia, miR-34a alterations have been described both in association with and independent of p53 deletions.

A role for miR-34a in normal hematopoiesis has not yet been defined. Such a role has been described for many miRNAs, with multiple recent studies describing the impact of miRNAs on lineage determinations during hematopoietic differentiation (reviewed in (Baltimore et al., 2008)). Indeed, these were some of the first functions described for miRNAs in mammalian systems, with miR-181 promoting B-lineage differentiation (Chen et al., 2004). The functional effects of miRNAs may depend on the regulation of a few critical factors that control gene expression, thereby affecting lineage choice (Xiao and Rajewsky, 2009). The range of targets ascribed to miR-34a suggests that it might have a role in the regulation of hematopoietic development. In fact, a role in B cell development was hypothesized following the demonstration that Bcl-2 is a direct target of miR-34a regulation (Bommer et al., 2007). It was particularly striking that an imbalance between Bax and Bcl-2 could lead to a defect in pro-B cell apoptosis in *Trp53*$^{-/-}$ mice. Here, we attempt to understand how miR-34a may be involved in hematopoiesis. We found that constitutive expression of miR-34a causes a partial block in B cell development, while its knockdown resulted in increased B cells. The key mediator of the miR-34a effect appears to be the Foxp1 transcription factor, which we showed to be a direct target of miR-34a. Knockdown of Foxp1 with an siRNA mimicked the effect of overexpression of miR-34a. Thus miR-34a appears to play an important role in the orchestration of B cell development in the mouse.

Results

Constitutive expression of miR-34a in the bone marrow leads to a decrease of B lymphocytes

To explore the role of miR-34a in hematopoietic differentiation, we designed retroviral vectors that express the microRNA. The vector co-expresses miR-34a and green fluorescent protein (GFP) and exploits the miR-155 format vector that we have previously utilized successfully to give strong expression of microRNA and siRNA (Fig 1A and (O'Connell et al., 2009)). The vector produced pre-miR-34a and mature miR-34a as demonstrated by RNA blotting (Fig 1B) or RT-qPCR (Supp Fig 1A), in addition to GFP (Supp Fig 1B). After transduction of murine bone marrow cells with miR-34a and control vectors followed by reconstitution of lethally irradiated syngeneic C57/B6 mice, we analyzed the recipient's bone marrow 2 months later. GFP positive cells were readily observed in both the control and miR-34a-transduced marrow recipients (hereafter referred to as "miR-34a mice"; Fig 1C). Expression of miR-34a was found to be elevated in primary bone marrow cells from the miR-34a mice (Fig 1D). The bone marrow was stained with a combination of antibodies to delineate the various hematopoietic lineages, including mature B cells (defined as being $CD19^{+}IgM^{+}$), myeloid cells ($CD11b^{+}$), T cells ($CD3\varepsilon^{+}$), and erythroid precursors ($Ter119^{+}$). A significant reduction in mature B cells, as a proportion of transduced cells (approximately 30% lower), was observed (Fig 1E). We did not observe statistically significant changes in myeloid cells (Fig 1F), erythroid precursors (Fig 1G) or T cells (Fig 1H). These differences were observed consistently across three experiments. Thus, constitutive expression of miR-34a causes a specific reduction in the number of mature B cells.

miR-34a expression results in a block in B cell development at the pro-B to pre-B cell stage in the bone marrow

To determine whether the observed reduction in mature B cells was the consequence of a specific developmental abnormality in B cell ontogeny, flow cytometric analyses were performed to delineate the various stages of B cell maturation. We found a significant (approximately two-fold) increase in pro-B cells ($CD19^{+}c\text{-}kit^{+}IgM^{-}$) in miR-34a mice (Fig 2A). Conversely, there was a significant reduction in pre-B cells ($B220^{+}CD43^{-}IgM^{-}$) in miR-34a mice (Fig 2B). This pattern indicates a developmental retardation at the pro-B to pre-B transition when B cells are passing through the pre-BCR checkpoint. A similar trend was observed when alternate stains were used to delineate pro-B cells (including $CD19^{+}CD43^{+}AA4.1^{+}$ and $CD43^{+}B220^{+}IgM^{-}$) and pre-B cells ($CD19^{+}CD25^{+}IgM^{-}$; data not shown). The numbers of pro- and pre-B cells in miR-34a mice correlated inversely with the expression pattern of miR-34a in the normal B-lineage cells, where relatively high miR-34a was observed at the pro-B cell stage with lower amounts in pre-B cells (Fig 2C). A second miR-34a expressing vector, which uses the native stem-loop structure and flanking regions and produces mature miR-34a at lower amounts, induced a similar phenotype (Supplemental Figure 2A, 2C and 2D). The decrease in bone marrow B cells resulted in decreased circulating B lymphocytes (Fig 2D), but splenic populations of B cells were largely restored in miR-34a overexpressing mice (Fig 2E). This likely represents homeostatic expansion of B cells in the periphery by mechanisms that are independent of miR-34a expression. Thus interrupting the physiological downregulation of miR-34a by constitutive expression results in a partial block in B-cell development.

Foxp1 is a bona fide target of miR-34a

To understand what targets of miR-34a might mediate the B cell developmental block, we examined predicted targets using the TargetScan database (Lewis et al., 2005). From this list of targets, we identified Foxp1, which is predicted to have two 7-mer sites in the 3′UTR. Because *Foxp1* has previously been implicated in B cell development, we examined whether

this gene is a target of miR-34a. The 3′UTR of *Foxp1* is schematically represented in Fig. 3A, showing the more 5′ of the 2 conserved miR-34a sites. To determine if Foxp1 might represent a direct target of miR-34a, luciferase assays were performed as previously described (O'Connell et al., 2008). Cells co-transfected with pcDNA3-miR-34a and luciferase linked to the *FOXP1*-3′UTR showed repression of luciferase compared to control (Fig 3B). When the conserved site in the *FOXP1* 3′UTR was mutated (as depicted in Fig 3A), luciferase expression was derepressed (Figure 3B; FOXP1mt). As controls, we examined repression of a UTR containing two repeats of the antisense sequence to miR-34a (2 repeats of antisense 22-mer), which showed the greatest repression (Fig 3B, a.s. 2mer), as well as repression of a *BCL2*-3′UTR containing construct, a previously reported miR-34a target (Fig 3B; BCL2 and BCL2mt;(Bommer et al., 2007)). As negative controls, we utilized the 3′UTR of two genes, *Cebpb* (encoding CEBPβ) and *Sfpi1* (encoding PU.1), which were repressed by miR-155, as well as a control luciferase construct with no UTR (Fig 3B, (O'Connell et al., 2008)). We have also examined the second UTR site which does not show repression in a similar assay (data not shown).

To examine the effects of miR-34a expression on endogenous Foxp1, we utilized two cell lines at a similar stage of differentiation- NALM6, which is a human pre-B cell line, and 70Z/3, which is a murine pre-B cell line. First, we assayed NALM6 single cell clones that had been transduced with a lentivector expressing miR-34a (Supp Fig 1C). This vector expressed GFP as well as miR-34a by RNA blot analysis and RT-qPCR (Supp Fig 1D–F). Analysis of the single cell clones revealed repression of *FOXP1* and overexpression of miR-34a RNA (Figure 3C and 3D, respectively). In murine 70Z/3 cells, we observed a similar repression of Foxp1 at the protein level within 4 days of transduction (Fig 3E). Analysis of Foxp1 RNA in B cell subsets showed an inverse correlation with miR-34a amounts at the pro- and pre-B cell stages (Fig 3F; compare with Fig 2C). Having observed repression of Foxp1 in cell lines, we also examined *Foxp1* mRNA expression in whole bone marrow from miR-34a mice. *Foxp1* mRNA is significantly downregulated in the bone marrow of mice transduced with miR-34a (Fig 3G), with no significant change observed in L32 control RNA (Fig 3H). It is notable that this difference was observed in whole bone marrow, where only about half of the cells had been transduced with miR-34a. Hence, repression of Foxp1 by miR-34a is demonstrated in human and mouse cell lines, as well as in primary murine bone marrow, and is mediated through a conserved site in the 3′UTR of *Foxp1*.

Direct repression of Foxp1 recapitulates constitutive miR-34a expression

Previous reports have indicated that the complete lack of Foxp1 results in a profound B cell developmental block that generates a near-total lack of mature B cells (Hu et al., 2006). To examine whether the phenotype of miR-34a expression might be explained by the repression of Foxp1, we developed constructs to express a siRNA against *Foxp1* (Foxp1si) in the same format as the construct expressing miR-34a (Fig 4A). Testing of this construct in 70Z/3 cells showed that *Foxp1* mRNA was repressed about 50%, similar to the repression observed in miR-34a-expressing cells (Fig 4B). In addition, repression by Foxp1si was similar to that by miR-34a at the protein level, where Foxp1 expression was reduced by about 50% (Fig 4B, right hand panel, compare to Fig 3E, right hand panel). Retroviral transduction and bone marrow transfer showed a high degree of reconstitution of the marrow by Foxp1si-expressing cells (Fig 4C). *Foxp1* RNA was reduced by about 50% in the marrow of mice reconstituted with this vector (Fig 4D). With this degree of repression, a dramatic increase in pro-B cells (about 3.5-fold) was observed (Fig 4E) along with a corresponding decrease in pre-B cells (Fig 4F). In contrast, retrovirally mediated knockdown of Bcl-2 in the bone marrow by a similar vector failed to recapitulate the phenotype observed in the miR-34a overexpressing mice, despite the demonstration that Bcl-2 is a direct target of miR-34a

(Supp Fig 3A and B). Instead, there were major reductions in all stages of B cell differentiation and a mild reduction in myeloid cells in the bone marrow (Supp Fig 3C, D, E, and F). Hence, the block in B cell development is largely recapitulated in a specific manner by the repression of Foxp1 using a siRNA.

Foxp1 cDNA lacking its 3′UTR is able to rescue the miR-34a mediated block in B cell development

Next, we tested whether complementation of Foxp1 by an exogenous cDNA not responsive to miR-34a could correct the B cell phenotype. MSCV based constructs containing the *Foxp1* coding sequence were generated with and without miR-34a as depicted in Figure 5A, and the vector containing both miR-34a and Foxp1 was designated as the “rescue vector”. These constructs contained the entire coding sequence of Foxp1, followed by an internal ribosomal entry sequence (IRES) to allow for GFP expression. The resultant constructs, when used to infect 70Z/3 cells, overexpressed Foxp1 at the protein level, at about 1.5–2 times endogenous levels (Fig 5B), and also overexpressed miR-34a (Fig 5C). Retroviral transduction and bone marrow transfer was completed as before, and we detected constitutive expression of *Foxp1* RNA by RT-qPCR (Fig 5D). In addition, miR-34a was constitutively expressed in mice receiving the rescue vector, Foxp1+34a, in a quantitatively similar manner to that observed when miR-34a was expressed by itself (Fig 5E). In the bone marrow, pro-B cell numbers were significantly decreased in animals receiving the rescue vector as compared to those receiving miR-34a alone, and similar to pro-B cell numbers observed in the mice receiving the control vector (Fig 5F). Similarly, pre-B cell numbers were comparable to those in control mice, with a significant increase in animals receiving the rescue vector compared with those animals receiving miR-34a alone (Fig 5G). These findings indicate that B cell maturation was largely rescued by provision of *Foxp1* lacking its 3′UTR in murine bone marrow. In contrast, such an effect was not observed when *BCL2* was utilized in a similar “rescue experiment” (constructs depicted in Supp Fig 5A). Despite BCL2 being a direct target of miR-34a and the detection of transduced *BCL2* in the bone marrow, the number of pro-B cells remained elevated, and the number of pre-B cells did not increase (Supp Fig 5 B,C,D, and E). Hence, the dependence of the miR-34a mediated B cell phenotype on Foxp1 is demonstrated in both loss-of-function and rescue contexts, indicating that Foxp1 is a highly specific target of miR-34a during B cell differentiation.

Knockdown of miR-34a results in increased numbers of mature B cells in the bone marrow

Our next step in understanding the role of miR-34a in B cells was to analyze the effects of miR-34a loss of function. We did this by attaching a so-called “sponge” sequence to a reporter (Gentner et al., 2009). In this approach, four consecutive synthetic miR-34a target sequences separated by four 4-6-nucleotide spacer sequences were cloned downstream of GFP in the previously described MGP vector (MGP-anti-34as; Fig 6A and Supplemental Table). Retrovirus generated from this construct was used to transduce 70Z/3 cells, which were immunoblotted for Foxp1. The cells expressing anti-34as showed an approximately 1.4-fold derepression of Foxp1 at the protein level (Fig 6B and data not shown). Luciferase assays performed using synthetic 34a target sites (ie., a perfectly complementary sequence; 34a-2mer) as well as the Foxp1 3′UTR in the reporter constructs demonstrated derepression as a consequence of expression of anti-34as (Fig 6C and 6D, respectively). This derepression was seen both as an effect on endogenous miR-34a activity (left two bars in Figs. 6C and 6D) and an effect on exogenously overexpressed miR-34a (right two bars in Figs. 6C–6D). The derepression was specific in that no derepression was seen if there was no UTR in the reporter plasmid or an irrelevant UTR (Fig 6E and data not shown). Next, we utilized this construct in a bone marrow transfer experiment, and found reproducible GFP expression in the recipient mice 2 months after transfer (Fig 6F). Examination of the bone marrow revealed an increase in the mature B cell population in mice with miR-34a

knockdown (Fig 6G versus 6H). These differences were statistically significant (Fig 6I). Minor differences were seen in the pro-B and pre-B cell populations, but these were not significant. In the bone marrow of mice transduced with anti-34as, Foxp1 RNA levels were modestly, but significantly derepressed (Fig 6J). This set of findings is best explained by the fact that pro-B and pre-B cells are transient states during B cell development-cells flux through these states, accumulating as mature B cells. The numbers of cells in these transient compartments in miR-34a knockdown mice are therefore not a sensitive measure of how rapidly cells are moving through the compartment whereas the number of mature B cells is a more sensitive measure. Because Foxp1 RNA levels seem so important in determining the course of B cell development, we analyzed pooled data from two experiments in which we overexpressed Foxp1 (see Fig 5), finding that indeed, it is the mature B cell pool (CD19+IgM+) that is increased upon modest overexpression of Foxp1 (Fig 6K). Thus, miR-34a knockdown causes a phenotype that is the opposite of that seen with constitutive expression, suggesting a role for miR-34a in the physiological regulation of B cell development.

Discussion

We describe here a role for miR-34a in B cell development that is largely explained by its repression of Foxp1. The block induced by miR-34a specifically involves Foxp1 because it is rescued by Foxp1 expression and not expression of another miR-34a target, BCL2. In early B cell development, loss of Foxp1 is known to cause a block at the pro-B cell to pre-B cell transition, and a near complete absence of B-lymphocytes in the peripheral lymphoid tissues (Hu et al., 2006). Additionally, Foxp1 downregulation is essential to monocytic differentiation, indicating a role in directing hematopoietic progenitors towards a B cell fate and away from the myeloid fate (Shi et al., 2008; Shi et al., 2004). By partial repression of Foxp1 in the bone marrow, constitutive miR-34a expression slows passage through the pro-B cell to pre-B cell transition, resulting in a lower number of circulating B cells. Conversely, loss of miR-34a function results in increased numbers of mature B cells (accompanied by modestly elevated amounts of Foxp1), implying a less stringent or faster transit through this checkpoint. The role of miR-34a and Foxp1 seem to be in controlling the output of the B cell developmental pathway, with mature B cells being the most sensitive measure of increased flux through this pathway. In differentiated B cells, *FOXP1* appears to act as a B cell oncogene, whose dysregulated expression can be a consequence of translocations to the *IGH* locus, in cases of marginal zone lymphoma, and through amplification in many cases of diffuse large B cell lymphoma (Lenz et al., 2008; Streubel et al., 2005; Wlodarska et al., 2005). Thus, Foxp1 is both needed for B cell differentiation and a danger in mature B cell life. We speculate that the effects of miR-34a on Foxp1 may be the mode through which p53 suppresses this potentially oncogenic protein in post-germinal center B cells. Such an effect would parallel the previously described role of miR-34a as a direct connection between the tumor suppressor p53 and the oncogenic protein Bcl-2.

The effect of miR-34a on the B cell developmental pathway is consistent with previously reported abnormalities seen with a deficiency of p53, namely an increased number of pre-B cells as well as B cells, with the latter finding also a consequence of loss of miR-34a function (Lu and Osmond, 2000). With miR-34a constitutively expressed, we find the opposite- an increase in pro-B cells and a decrease in pre-B and B cells. Our findings imply a connection between p53 and Foxp1 via the action of miR-34a. In early B cell development, Foxp1 activates several B cell factors, such as E2a and Pax-5 and binds to the enhancers of the *Rag* genes (Hu et al., 2006). This activity of Foxp1 may be dependent on the downregulation of miR-34a, releasing repression of Foxp1, and allowing B cell development to proceed. We interrupt this physiological downregulation by constitutive expression, resulting in an accumulation of pro-B cells. With miR-34a loss-of-function,

mature B cells are increased, likely arising from the loss of a miR-34a dependent checkpoint. The idea that Foxp1 expression is important for the output of B cells from the bone marrow is borne out by the following: (i) reciprocal changes in Foxp1 levels with miR-34a gain- and loss-of-function, (ii) mature B cells are increased in the marrow of mice that overexpress Foxp1 and (iii) a partial arrest at the pro-B to pre-B transition is found in Foxp1si-expressing mice.

The effects of miRNAs in B cell development have been assessed globally as well as in terms of specific miRNAs. The deletion of Dicer at the earliest stages of B cell development leads to a block in development at the pro-B to pre-B transition (Koralov et al., 2008). In this case, bioinformatic analysis showed that upregulated genes in Dicer-deficient B-lineage cells were likely those targeted by the miR-17~92 cluster, and that ablation of the pro-apoptotic protein Bim (a target of miR-17~92) or transgenic overexpression of Bcl-2 could partially rescue the developmental block. This target specificity is distinct from the block induced by miR-34a, because Bcl-2 increased survival of miR-34a expressing pro-B cells but did not significantly promote their differentiation. B cell developmental blocks have also been seen following the disruption of specific miRNAs. Early expression of miR-150 led to a block in B cell development, while its deletion led to expansions of certain B cell subsets (Xiao et al., 2007; Zhou et al., 2007). In this case, the relevant target appeared to be c-Myb, a transcription factor involved in many stages of lymphocyte differentiation. Overexpression of the miR-17~92 cluster led to a B-lymphoproliferative disease, likely as a consequence of suppression of the tumor suppressor gene PTEN and Bim (Xiao et al., 2008). Other miRNAs with effects of B cell development include miR-181a and miR-155, which promote early B cell development and the germinal center response, respectively (Chen et al., 2004; Rodriguez et al., 2007; Thai et al., 2007; Vigorito et al., 2007). Specific targeting by miR-155 in the context of B cell development has been extensively investigated and it appears that multiple targets are responsible for miR-155-induced phenotypes (Chen et al., 2008; Pedersen et al., 2008; Vigorito et al., 2007).

The specificity of miRNA targeting remains incompletely understood. On the one hand, miRNAs, including miR-34a, are predicted to target hundreds of genes by computational algorithms. On the other hand, in particular developmental contexts, one or a few genes are most important in the causation of a miRNA-mediated phenotype. Such observations have been made in both loss-of-function and gain-of-function contexts, indicating the general applicability of this principle for particular miRNAs. Our study extends these observations by demonstrating a specificity of miR-34a targeting for Foxp1 in early B-lymphoid development. This is based on both recapitulation and rescue of the phenotype by Foxp1 loss- and gain-of-function, respectively. The basis of such specificity is likely the fact that certain cell fate decisions hinge on small changes in the expression of critical lineage specification genes, and miRNAs can cause such changes. From this, it can be inferred that the study of miRNAs in hematopoietic development may illuminate critical points in cell fate decisions, and bring novel insights into this complex and dynamic developmental system.

Our findings may be of relevance in human disease as others have observed that miR-34a is functionally lost (either directly or as a consequence of p53 deletion) in chronic lymphocytic leukemia but is overexpressed in acute myeloid leukemia (Isken et al., 2008; Mraz et al., 2009; Zenz et al., 2009). In our study overexpression of miR-34a led to disruptions in B cell development, but not myeloid development. We have confirmed independently that miR-34a is overexpressed in AML by RT-qPCR (data not shown) and that its overexpression does not correlate with that of miR-155. Since we did not observe a myeloproliferative disorder in miR-34a-overexpressing mice, any mechanism whereby miR-34a contributes to leukemia is likely to be distinct from that observed in miR-155

expressing mice (O'Connell et al., 2008). Our findings suggest one possibility- the expression of miR-34a may affect the phenotype of the leukemic cells by blocking cells transformed by other oncogenic lesions from differentiating into B- lineage cells. Indeed, some recent studies indicate that there may be a progenitor with lymphoid characteristics that gives rise to acute myeloid leukemia (Deshpande et al., 2006). Our results suggest that miRNA expression may be one mechanism whereby the leukemia assumes a distinctive lymphoid or myeloid phenotype. Such phenotypic specification certainly has clinical relevance, as acute myeloid leukemia in general remains the more difficult of the acute leukemias to treat. However, further work needs to be done to understand the role that miR-34a plays in leukemia and how its action or inhibition can be parlayed into novel therapeutic strategies.

Materials and Methods

Cell Culture

All cells were cultured in a sterile incubator maintained at 37°C with 5% CO_2. 293T cells were cultured in complete DMEM with 10% FBS, 100 units/ml penicillin and 100 units/ml streptomycin. WEHI-231 and 70Z/3 cells were cultured in complete RPMI with 10% FBS, 100 units/ml penicillin, 100 units/ml streptomycin and 50 μM 2-Mercaptoethanol.

DNA constructs

The MGP vector system has been described previously, and further detailed cloning strategies are available upon request (O'Connell et al., 2009). Table S1 contains sequence information for all oligonucleotides used to build new constructs. MiR-34a and siRNAs were built using the Invitrogen BlockiT pol II miR RNAi strategy as described previously, using the miR-155 arms for processing (O'Connell et al., 2009). SiRNA sequences were predicted using the Invitrogen BlockiT miR RNAi designer. In addition, a 300-base pair sequence of human genomic DNA encoding the native miR-34a mature sequence, endogenous stem-loop structure and flanking sequences was PCR-amplified using the 34a.NotI.f and 34a.XhoI.r primers and cloned into the MGP vector using the NotI and XhoI sites, as well as into pcDNA3 using 34a.EcoRI.f and 34a.XhoI.r primers and cloning into the EcoRI and XhoI sites. The MGP-based vector is referred to as MGP-miR-34a-lo. The last set of expression vectors, utilized for expression of miR-34a in human cell lines, was developed from the FUGW vector system (Lois et al., 2002). For this purpose, miR-34a genomic sequence was cut out of pcDNA3-34a and blunt-ligated into the FUGW EcoRI site. For reporter assays, two regions of the *FoxP1* 3′ UTR were amplified by PCR, each containing a putative miR-34a binding site as determined by TargetScan (Lewis et al., 2005). The 5′ segment was 637 base pairs and the 3′ segment was 760 base pairs. 2000 base pairs of the *BCL2* 3′ UTR was also PCR-amplified. These PCR products were cloned into pmiReport (Ambion, Austin, TX). The miR-34a seed regions in both the *FoxP1* 3′UTR 5′ segment and the *BCL2* 3′ UTR segment were mutated using PCR to yield Foxp1mt and BCL2mt constructs. A positive control insert consisting of two miR-34a antisense sites (antisense 2-mer) was constructed by annealing oligonucleotides with SpeI and HindIII sticky ends and cloning into pmiReport. For the rescue vectors, cDNAs for *Foxp1* and *BCL2* were PCR-amplified from pCMV-Sport-Foxp1 (Open Biosystems) and pDNR-Dual-BCL2 (Harvard PlasmID Core Facility), and cloned between the BglII and XhoI sites in MSCV-IRES-GFP, yielding MIG/Foxp1 and MIG/BCL2, respectively. The cDNAs contain the entire coding sequence for Foxp1 (listed in supplemental table 1) and BCL2, respectively. miR-34a was cloned by PCR amplification from pcDNA3-34a and cloned between the XhoI and EcoRI sites in the MIG vectors, yielding MIG/Foxp1+34a and MIG/BCL2+34a vectors respectively. The MGP/anti-34as construct was generated by annealing the 34a-spacer-f and 34a-spacer-r oligonucleotides (designed with XhoI/NotI sticky ends) and ligating into the

MGP vector with XhoI and NotI. The spacers between each miR-34a binding site were the same as those previously published (Gentner et al., 2009).

Mice and Bone marrow reconstitution experiments

C57BL/6 mice were bred and housed in the Caltech Office of Laboratory Animal Resources (OLAR) facility. The Caltech Institutional Animal Care and Use Committee (IACUC) approved all experiments related to mice. Virus production and reconstitution experiments were performed as previously described (O'Connell et al., 2008). Experimental groups of 4–5 mice received each of the vectors described. Recipient mice were monitored for health and a peripheral blood sample removed at 1 month for flow cytometric analysis. Mice were sacrificed 2 months after reconstitution and were examined by morphology, FACS and RT-qPCR as described below. All experiments were repeated at least twice and in most cases, 3 times, as described in figure legends.

Flow cytometry

Cells were isolated from the relevant tissue, homogenized, and red blood cells were lysed using RBC lysis buffer (Biolegend). Cells were stained with the following Fluorophore-conjugated antibodies (all from Ebioscience): CD3ε, CD11b, CD19, B220, CD43, CD117 (c-kit), CD25, IgM, Gr-1, Ter-119, AA4.1, CD4, and CD8α, in various combinations to delineate the hematopoietic lineages and various stages of B cell differentiation. Cells were sorted using a FACSCalibur (Becton Dickinson) and all data were analyzed using FloJo software (Treestar). Specific gating strategies to delineate various B cell populations are available upon request. Data were presented as the percentage of GFP positive cells in the relevant hematopoietic compartment. These data were also compared against the GFP-negative cells within the same mouse.

Cell sorting for RNA analysis at various stages of B cell differentiation

Bone marrows were extracted from 2 mice, lysed in RBC lysis buffer, and spun down. Cells were then resuspended in lymphocyte FACS buffer (1X Hanks Buffered Salt Solution, 10mM HEPES, 2.5 mg/mL BSA), filtered through a 40μm mesh, blocked with FcBlock (Becton Dickinson), and depleted on a magnetic column for CD11b, Gr-1, Ter119, CD3ε, and NK1.1 using biotinylated antibodies and streptavidin-MACS beads, as per manufacturer's instructions (Miltenyi). Cells were then stained with c-kit, B220, CD43, IgM, Streptavidin, and CD138, and sorted on a BD Biosciences FACSVantage flow cytometer (Caltech Core facility). 4 populations of cells were collected: Lin- (B220-, IgM-, Streptavidin-, and CD138-); pro-B cells (c-kit+B220+CD43+IgM-streptividin-), pre-B cells (B220+CD43-c-kit-IgM-streptavidin-) and B cells (B220+c-kit-CD43-IgM+strepatavidin-). RNA was isolated by TRIzol (Invitrogen) purification and subjected to RT-qPCR as described below. These sorts were repeated three times, with similar results.

Sequence alignments

The miR-34a seed region and Foxp1 3′ UTR sequences from human (*Homo sapiens*), mouse (*Mus musculus*), rat (*Rattus norvegicus*) and dog (*Canis familiaris*) were obtained and aligned using TargetScan (Lewis et al., 2005).

Experiments with cell lines

VSV-G-pseudotyped FUGW lentiviruses were made using TransIT-293 based transient transfections of 293T cells. The viruses were then used to infect NALM6 human pre-B cells by spin-infection at 1,200×g for 90 minutes at 30C, supplemented with 10μg/mL polybrene (Chemicon). Single cell clones were derived by subjecting the cells to limiting dilution assays. Clones were maintained in RPMI supplemented with 10% FBS and antibiotics. For

examination of Foxp1 levels in murine cells, MSCV-based retroviruses were prepared as described previously, pseudotyped with pCL-Eco, and used to infect 70Z/3 murine pre-B cells. Cells were expanded for 3–4 days, and then utilized for RNA purification or protein extraction for Western Blotting.

Luciferase Reporter assays

2×10^5 293T cells were cultured for 18 hours and subsequently transfected with relevant plasmids with TransIT 293. Transfected plasmids included pcDNA3, pcDNA3-34a, β-gal expression vector, and pmiReport vectors. For the derepression assays with the sponge construct, we added in MGP (empty vector) or MGP/anti-34as. After 48 hours, cells were lysed using Reporter Lysis Buffer (Promega, Madison, WI) and subjected to luciferase reporter assays as previously described (O'Connell et al., 2008).

RNA preparation and quantitation

RNA was isolated using TRIzol as per manufacturer's instructions. SYBR Green based quantitative real-time PCR (qPCR) was performed using the 7300 Real-time PCR system (Applied Biosystems, Foster City, CA) to assay miR-34a, 5s, *FoxP1* mRNA, *BCL2* mRNA and L32 mRNA levels as described previously (O'Connell et al., 2008). Mature miR-34a and 5s RNA were assayed using a miRVana miRNA detection kit as per manufacturer's instructions (Ambion). Human *FOXP1*, *BCL2* and L32 mRNA were detected using specific primers and utilizing the SybrGreen system (Applied Biosystems) (Table S1).

Immunoblotting

Total cell extracts were fractionated by electrophoresis on 10% SDS polyacrylamide gel and electroblotted to Trans-Blot nitrocellulose membrane (Bio-Rad, Hercules, CA) using a semi-dry transfer apparatus (Bio-Rad). Protein detection was performed using the following antibodies: FoxP1 (ab16645) (Abcam, Cambridge, MA), β-Actin (A1978) (Sigma, St. Louis, MO); GAPDH (sc-47724), α-Tubulin (sc-5286), goat anti-mouse HRP-conjugated secondary antibody (sc-2005), goat anti-rabbit HRP-conjugated secondary antibody (sc-2004) (Santa Cruz Biotechnology, Santa Cruz, CA). Expression intensities were determined using Scion Image software.

Statistical tests

All statistical analyses were performed using Microsoft Excel. Expression and flow cytometric data were first analyzed by an F-test to determine whether the distributions were homo- or heteroscedastic. Then, the correct type of unpaired, two-tailed T-test was applied to determine if the distributions were statistically different. T-tests that returned p-values of less than 0.05 were considered to be statistically significant.

Supplementary Material

Refer to Web version on PubMed Central for supplementary material.

Acknowledgments

We would like to thank members of the Baltimore laboratory, Dr. Kenneth Dorshkind, and Dr. Ellen Rothenberg for helpful discussions. This work was supported by career development award 1K08CA133521 from the National Cancer Institute and a clinical fellowship training grant from the California Institute of Regenerative Medicine/Eli and Edythe Broad Center for Regenerative Medicine and Stem cell Research at UCLA (D.S.R.), the Irvington Institute Fellowship Program of the Cancer Research Institute (R.M.O.), the graduate research fellowship program of the National Science Foundation (A.A.C.), and National Institutes of Health (1R01AI079243-01; D.B.).

References

Alizadeh AA, Eisen MB, Davis RE, Ma C, Lossos IS, Rosenwald A, Boldrick JC, Sabet H, Tran T, Yu X, et al. Distinct types of diffuse large B cell lymphoma identified by gene expression profiling. Nature. 2000; 403:503–511. [PubMed: 10676951]

Baltimore D, Boldin MP, O'Connell RM, Rao DS, Taganov KD. MicroRNAs: new regulators of immune cell development and function. Nat Immunol. 2008; 9:839–845. [PubMed: 18645592]

Bommer GT, Gerin I, Feng Y, Kaczorowski AJ, Kuick R, Love RE, Zhai Y, Giordano TJ, Qin ZS, Moore BB, et al. p53-Mediated Activation of miRNA34 Candidate Tumor-Suppressor Genes. Curr Biol. 2007; 17:1298–1307. [PubMed: 17656095]

Busslinger M. Transcriptional control of early B cell development. Annu Rev Immunol. 2004; 22:55–79. [PubMed: 15032574]

Chang TC, Wentzel EA, Kent OA, Ramachandran K, Mullendore M, Lee KH, Feldmann G, Yamakuchi M, Ferlito M, Lowenstein CJ, et al. Transactivation of miR-34a by p53 broadly influences gene expression and promotes apoptosis. Mol Cell. 2007; 26:745–752. [PubMed: 17540599]

Chen CZ, Li L, Lodish HF, Bartel DP. MicroRNAs modulate hematopoietic lineage differentiation. Science. 2004; 303:83–86. [PubMed: 14657504]

Chen L, Cui B, Zhang S, Chen G, Croce CM, Kipps TJ. Association Between the Proficiency of B cell Receptor Signaling and the Relative Expression Levels of ZAP-70, SHIP-1, and Mir-155 in Chronic Lymphocytic Leukemia. Blood. 2008; 112:3155.

Deshpande AJ, Cusan M, Rawat VP, Reuter H, Krause A, Pott C, Quintanilla-Martinez L, Kakadia P, Kuchenbauer F, Ahmed F, et al. Acute myeloid leukemia is propagated by a leukemic stem cell with lymphoid characteristics in a mouse model of CALM/AF10-positive leukemia. Cancer Cell. 2006; 10:363–374. [PubMed: 17097559]

Gentner B, Schira G, Giustacchini A, Amendola M, Brown BD, Ponzoni M, Naldini L. Stable knockdown of microRNA in vivo by lentiviral vectors. Nat Methods. 2009; 6:63–66. [PubMed: 19043411]

Guidos CJ, Williams CJ, Grandal I, Knowles G, Huang MT, Danska JS. V(D)J recombination activates a p53-dependent DNA damage checkpoint in scid lymphocyte precursors. Genes Dev. 1996; 10:2038–2054. [PubMed: 8769647]

Hardy RR, Hayakawa K. B cell development pathways. Annu Rev Immunol. 2001; 19:595–621. [PubMed: 11244048]

He L, He X, Lim LP, de Stanchina E, Xuan Z, Liang Y, Xue W, Zender L, Magnus J, Ridzon D, et al. A microRNA component of the p53 tumour suppressor network. Nature. 2007; 447:1130–1134. [PubMed: 17554337]

Hermeking H. The miR-34 family in cancer and apoptosis. Cell Death Differ. 2009

Hu H, Wang B, Borde M, Nardone J, Maika S, Allred L, Tucker PW, Rao A. Foxp1 is an essential transcriptional regulator of B cell development. Nat Immunol. 2006; 7:819–826. [PubMed: 16819554]

Isken F, Steffen B, Merk S, Dugas M, Markus B, Tidow N, Zuhlsdorf M, Illmer T, Thiede C, Berdel WE, et al. Identification of acute myeloid leukaemia associated microRNA expression patterns. Br J Haematol. 2008; 140:153–161. [PubMed: 18173753]

Koralov SB, Muljo SA, Galler GR, Krek A, Chakraborty T, Kanellopoulou C, Jensen K, Cobb BS, Merkenschlager M, Rajewsky N, Rajewsky K. Dicer ablation affects antibody diversity and cell survival in the B lymphocyte lineage. Cell. 2008; 132:860–874. [PubMed: 18329371]

Lenz G, Wright GW, Emre NC, Kohlhammer H, Dave SS, Davis RE, Carty S, Lam LT, Shaffer AL, Xiao W, et al. Molecular subtypes of diffuse large B cell lymphoma arise by distinct genetic pathways. Proc Natl Acad Sci U S A. 2008; 105:13520–13525. [PubMed: 18765795]

Lewis BP, Burge CB, Bartel DP. Conserved seed pairing, often flanked by adenosines, indicates that thousands of human genes are microRNA targets. Cell. 2005; 120:15–20. [PubMed: 15652477]

Lewis BP, Shih IH, Jones-Rhoades MW, Bartel DP, Burge CB. Prediction of mammalian microRNA targets. Cell. 2003; 115:787–798. [PubMed: 14697198]

Lois C, Hong EJ, Pease S, Brown EJ, Baltimore D. Germline transmission and tissue-specific expression of transgenes delivered by lentiviral vectors. Science. 2002; 295:868–872. [PubMed: 11786607]

Lu L, Osmond DG. Apoptosis and its modulation during B lymphopoiesis in mouse bone marrow. Immunol Rev. 2000; 175:158–174. [PubMed: 10933601]

Meffre E, Casellas R, Nussenzweig MC. Antibody regulation of B cell development. Nat Immunol. 2000; 1:379–385. [PubMed: 11062496]

Mraz M, Malinova K, Kotaskova J, Pavlova S, Tichy B, Malcikova J, Stano Kozubik K, Smardova J, Brychtova Y, Doubek M, et al. miR-34a, miR-29c and miR-17-5p are downregulated in CLL patients with TP53 abnormalities. Leukemia. 2009

O'Connell RM, Chaudhuri AA, Rao DS, Baltimore D. Inositol phosphatase SHIP1 is a primary target of miR-155. Proc Natl Acad Sci U S A. 2009

O'Connell RM, Rao DS, Chaudhuri AA, Boldin MP, Taganov KD, Nicoll J, Paquette RL, Baltimore D. Sustained expression of microRNA-155 in hematopoietic stem cells causes a myeloproliferative disorder. J Exp Med. 2008

Pedersen IM, Otero DC, Kao E, Sedy A, Hother C, Ralfkiaer E, Rickert RC, Gronbaek K, David M. Onco-Mir-155 Targets SHIP to Regulate TNF-Dependent B cell Lymphoma Growth. Blood. 2008; 112:604.

Raver-Shapira N, Marciano E, Meiri E, Spector Y, Rosenfeld N, Moskovits N, Bentwich Z, Oren M. Transcriptional activation of miR-34a contributes to p53-mediated apoptosis. Mol Cell. 2007; 26:731–743. [PubMed: 17540598]

Rodriguez A, Vigorito E, Clare S, Warren MV, Couttet P, Soond DR, van Dongen S, Grocock RJ, Das PP, Miska EA, et al. Requirement of bic/microRNA-155 for normal immune function. Science. 2007; 316:608–611. [PubMed: 17463290]

Shi C, Sakuma M, Mooroka T, Liscoe A, Gao H, Croce KJ, Sharma A, Kaplan D, Greaves DR, Wang Y, Simon DI. Down-regulation of the forkhead transcription factor Foxp1 is required for monocyte differentiation and macrophage function. Blood. 2008; 112:4699–4711. [PubMed: 18799727]

Shi C, Zhang X, Chen Z, Sulaiman K, Feinberg MW, Ballantyne CM, Jain MK, Simon DI. Integrin engagement regulates monocyte differentiation through the forkhead transcription factor Foxp1. J Clin Invest. 2004; 114:408–418. [PubMed: 15286807]

Shu W, Yang H, Zhang L, Lu MM, Morrisey EE. Characterization of a new subfamily of winged-helix/forkhead (Fox) genes that are expressed in the lung and act as transcriptional repressors. J Biol Chem. 2001; 276:27488–27497. [PubMed: 11358962]

Streubel B, Vinatzer U, Lamprecht A, Raderer M, Chott A. T(3;14)(p14.1;q32) involving IGH and FOXP1 is a novel recurrent chromosomal aberration in MALT lymphoma. Leukemia. 2005; 19:652–658. [PubMed: 15703784]

Thai TH, Calado DP, Casola S, Ansel KM, Xiao C, Xue Y, Murphy A, Frendewey D, Valenzuela D, Kutok JL, et al. Regulation of the germinal center response by microRNA-155. Science. 2007; 316:604–608. [PubMed: 17463289]

Vigorito E, Perks KL, Abreu-Goodger C, Bunting S, Xiang Z, Kohlhaas S, Das PP, Miska EA, Rodriguez A, Bradley A, et al. microRNA-155 regulates the generation of immunoglobulin class-switched plasma cells. Immunity. 2007; 27:847–859. [PubMed: 18055230]

Wang B, Weidenfeld J, Lu MM, Maika S, Kuziel WA, Morrisey EE, Tucker PW. Foxp1 regulates cardiac outflow tract, endocardial cushion morphogenesis and myocyte proliferation and maturation. Development. 2004; 131:4477–4487. [PubMed: 15342473]

Wlodarska I, Veyt E, De Paepe P, Vandenberghe P, Nooijen P, Theate I, Michaux L, Sagaert X, Marynen P, Hagemeijer A, De Wolf-Peeters C. FOXP1, a gene highly expressed in a subset of diffuse large B cell lymphoma, is recurrently targeted by genomic aberrations. Leukemia. 2005; 19:1299–1305. [PubMed: 15944719]

Xiao C, Calado DP, Galler G, Thai TH, Patterson HC, Wang J, Rajewsky N, Bender TP, Rajewsky K. MiR-150 controls B cell differentiation by targeting the transcription factor c-Myb. Cell. 2007; 131:146–159. [PubMed: 17923094]

Xiao C, Rajewsky K. MicroRNA control in the immune system: basic principles. Cell. 2009; 136:26–36. [PubMed: 19135886]

Xiao C, Srinivasan L, Calado DP, Patterson HC, Zhang B, Wang J, Henderson JM, Kutok JL, Rajewsky K. Lymphoproliferative disease and autoimmunity in mice with increased miR-17-92 expression in lymphocytes. Nat Immunol. 2008

Zenz T, Mohr J, Eldering E, Kater AP, Buhler A, Kienle D, Winkler D, Durig J, van Oers MH, Mertens D, et al. miR-34a as part of the resistance network in chronic lymphocytic leukemia. Blood. 2009; 113:3801–3808. [PubMed: 18941118]

Zhou B, Wang S, Mayr C, Bartel DP, Lodish HF. miR-150, a microRNA expressed in mature B and T cells, blocks early B cell development when expressed prematurely. Proc Natl Acad Sci U S A. 2007; 104:7080–7085. [PubMed: 17438277]

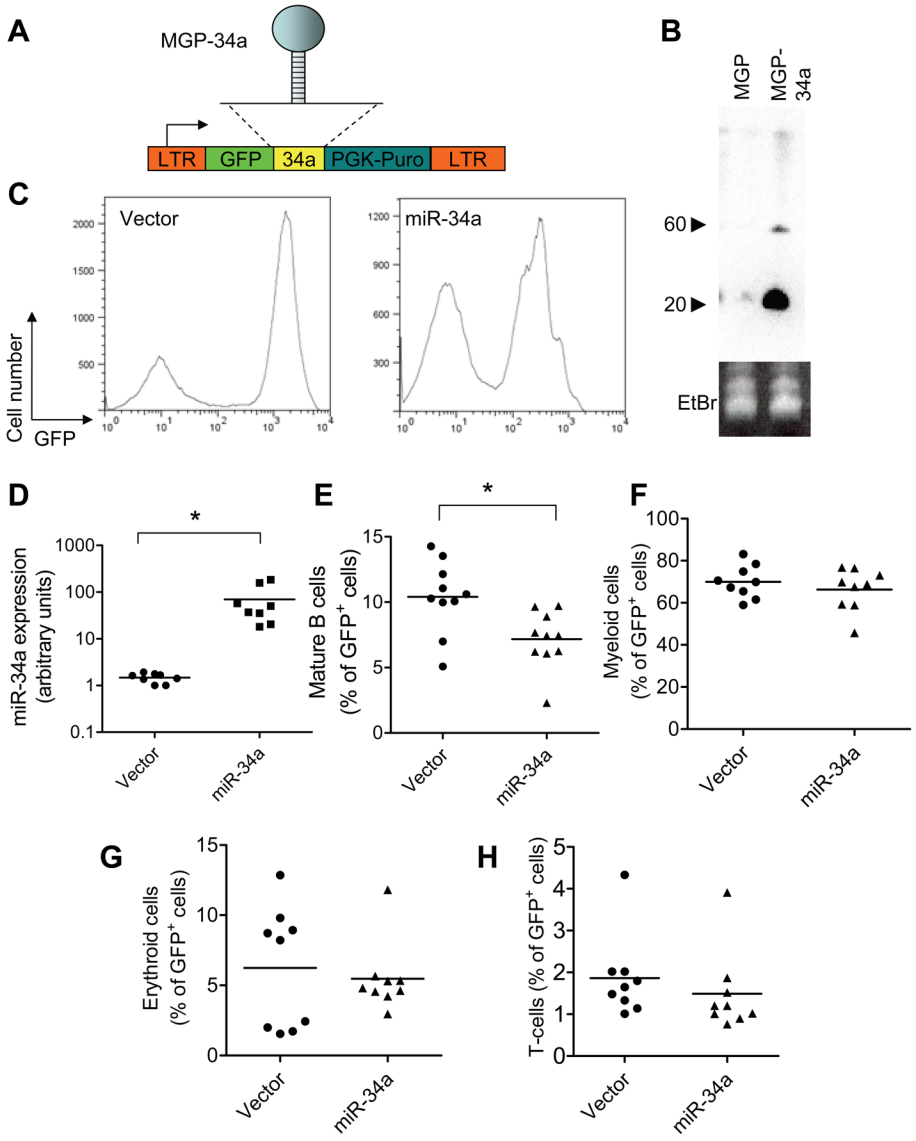

Figure 1. Constitutive expression of miR-34a in the bone marrow compartment leads to a decrease in mature B-lymphocytes

A. Schematic representation of the MSCV-based retroviral vector used to express miR-34a, based on the previously described MGP vector (O'Connell et al., 2009).

B. Expression of pre-miR-34a (~60nt) and mature miR-34a (~20nt) was assayed by RNA blotting. The bottom panel shows Ethidium bromide staining (EtBr) to confirm equal loading.

C. Analysis of GFP expression in bone marrow two months after retroviral transduction and transfer.

D. Expression of miR-34a in bone marrow by RT-qPCR, normalized by 5S. Individual dots represent one mouse; the lines show the mean of miR-34a expression in individual mice from two independent experiments (n=8 for each group; T-test, p=0.009).

E. Bone marrow mature B cells detected as a percentage of GFP^+ cells by flow cytometry in mice expressing vector alone or miR-34a are shown. Individual dot represents one mouse; the lines show the mean percentage of B-cells in individual mice from three independent experiments (n=10 for each group; T-test, p=0.0093).

F–H. Flow cytometric analyses for myeloid cells (defined as GFP^+CD11b^+), erythroid cells ($GFP^+Ter119^+$), and T cells ($GFP^+CD3\varepsilon^+$) are shown. Individual dots represent percent of myeloid cells (F), erythroid cells (G) and T cells (H) in the bone marrow of an individual mouse, and the bars show the mean percent of each cell type in mice from three independent experiments (n=9 for each group; T-test, n.s.).

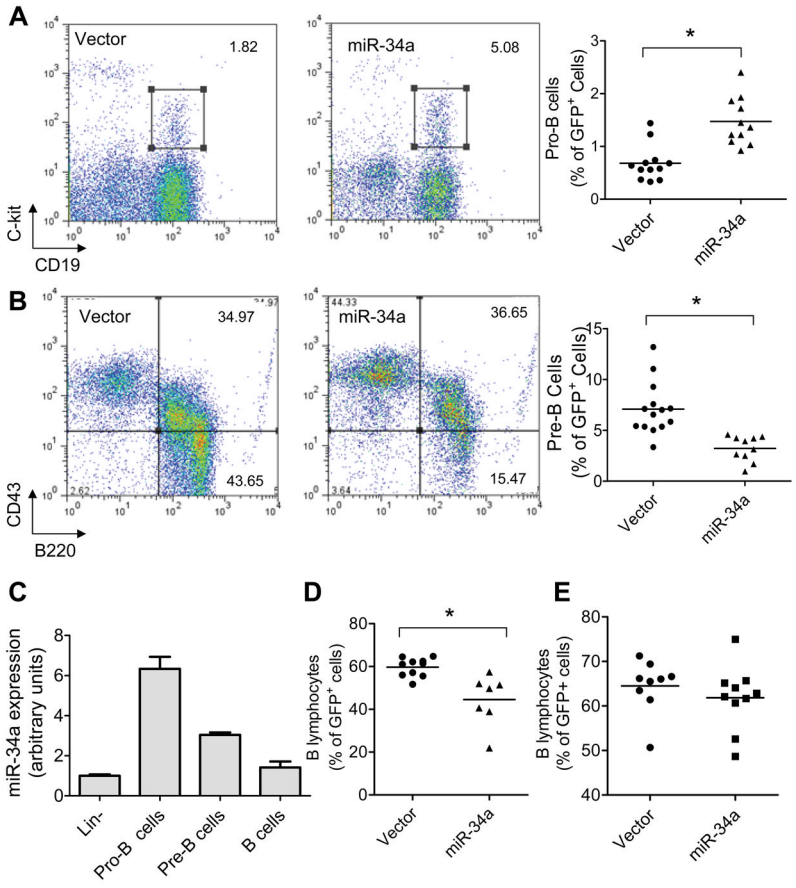

Figure 2. miR-34a expression causes an increase in pro-B cells and a decrease in pre-B cells

A. Analysis of pro-B cells. Bone marrow cells stained with CD19, c-kit and IgM, analyzed by flow cytometry. Left hand panels show representative histograms of the GFP^+IgM^- compartment in control (vector) and miR-34a expressing mice. In the right hand panel, individual dots represent the percent of pro-B cells in the bone marrow of an individual mouse, and the bars show the mean percent of pro-B cells in mice from three independent experiments (n=12 for control and n=10 for miR-34a mice; T-test, p=.0001).

B. Analysis of pre-B cells. Bone marrow cells stained with B220, IgM and CD43 were analyzed by flow cytometry. Left hand panels show representative histograms of the GFP^+IgM^- compartment in control and miR-34a expressing mice. In the right hand panel, individual dots represent the percent of pro-B cells in the bone marrow of an individual mouse, and the bars show the mean percent of pro-B cells in mice from three independent experiments (n=14 for control and n=10 for miR-34a mice; T-test, p=0.0002).

C. Assessment of miR-34a expression in B-lineage cells at various stages of differentiation collected by cell sorting. Bar graph shows mean + s.d. of miR-34a expression (n=2 samples; three independent experiments were analyzed).

D. Peripheral blood B-lymphocytes in control and miR-34a mice, with individual dots representing the percent of B-lymphocytes in individual mice and the bars showing the mean percent of B-cells from three independent experiments (n=11 for vector control and n=7 for miR-34a; p=0.02).

E. Enumeration of splenic B cells in miR-34a expressing mice. Individual dots represent the percent of B-cells amongst total spenocytes in individual mice; bars represent the mean percent of B-cells in mice from 3 independent experiments (n=9 for vector control and n=9 for miR-34a).

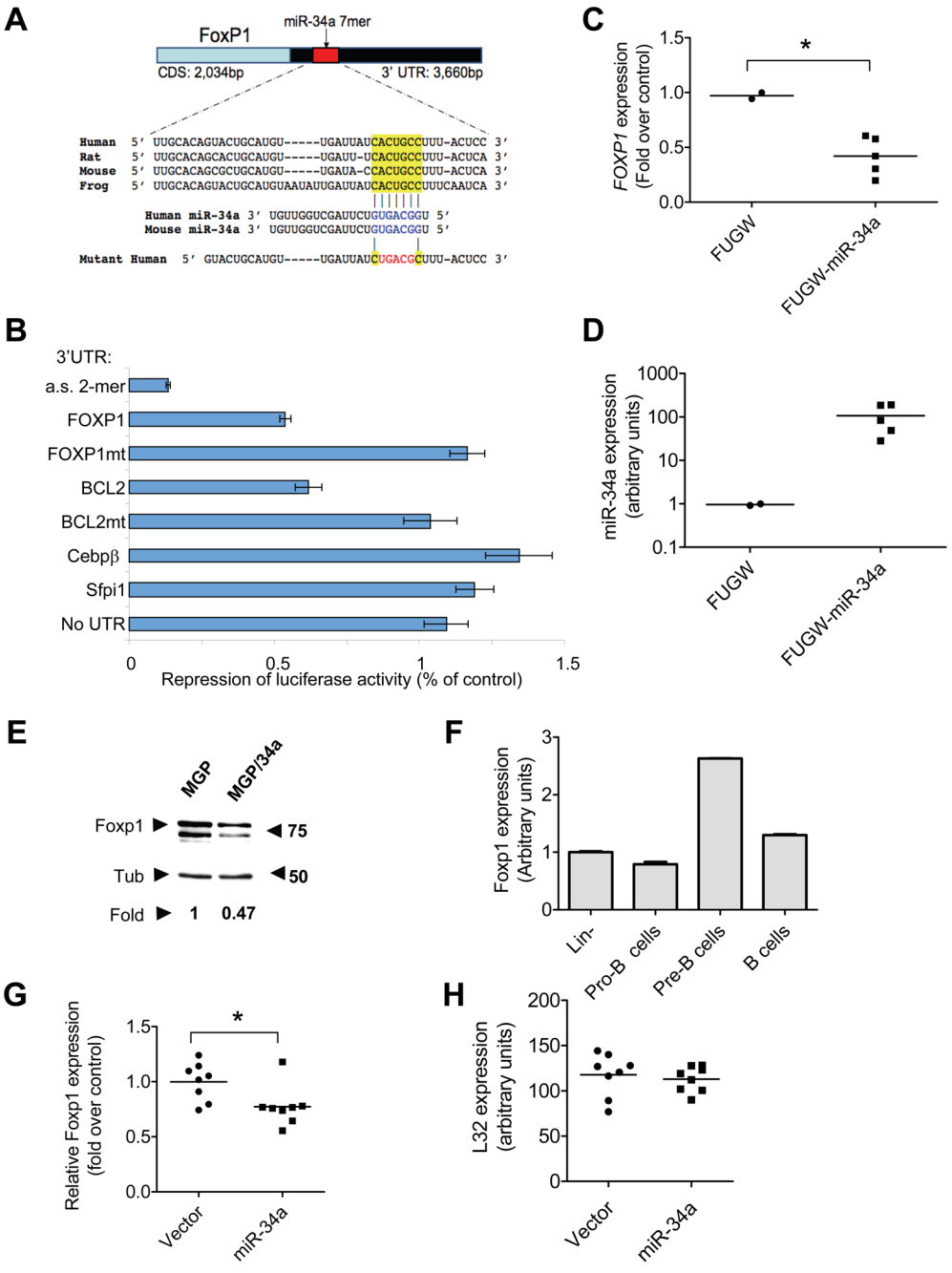

Figure 3. Foxp1 is a bona fide target of miR-34a

A. Schematic representation of *Foxp1* cDNA and 3′UTR showing the conserved miR-34a seed region in its 3′UTR. Human and mouse miR-34a mature sequences with proposed base pairing to the 3′UTR are presented as is the mutant 3′UTR used in the luciferase assays depicted in B.

B. Targeting of *Foxp1* by miR-34a is via direct 3′UTR interactions. Graphed is the relative luciferase activity of 293T extracts transfected with the designated luciferase-3′UTR construct and mir-34a compared to cells transfected with the luciferase-3′UTR and empty vector, normalized for transfection efficiency by a β-galactosidase reporter. Designations are for the various 3′UTRs attached to the luciferase reporter: a.s.2-mer, two copies of the

miR-34a anti-sense sequence; *FOXP1*mt, *FOXP1* 3′UTR with mutated mir-34a seed site; *BCL2*mt, *BCL2* 3′UTR with mutated mir-34a seed site; No UTR, luciferase gene without a 3′UTR.

C. *FOXP1* expression, measured by RT-qPCR in NALM6 clones that express control vector (FUGW) or miR-34a (FUGW/34a). Individual dots represent *FOXP1* RNA levels in individual clones, while the bars represent the mean values in each case (T-test, p=0.0086).

D. miR-34a expression, measured by RT-qPCR, in NALM6 clones as in (C).

E. Immunoblot analysis of of murine Foxp1 in 70Z/3 cells infected with MGP-34a versus vector alone. The numbers below the blot indicate the relative expression level of the protein as compared with the control. This experiment was repeated twice with similar results.

F. Assessment of *FOXP1* expression in B-lineage cells at various stages of differentiation collected by cell sorting. Bar graph shows mean + s.d. of FOXP1 expression (n=2 samples; two independent experiments were analyzed).

G. and H. *Foxp1* (G) and L32 (H) expression measured by RT-qPCR in the bone marrow of mice reconstituted with either vector- or miR-34a (n=7 for vector, n=8 for miR-34a). T-test, p=0.0225 for comparison of *Foxp1* expression levels.

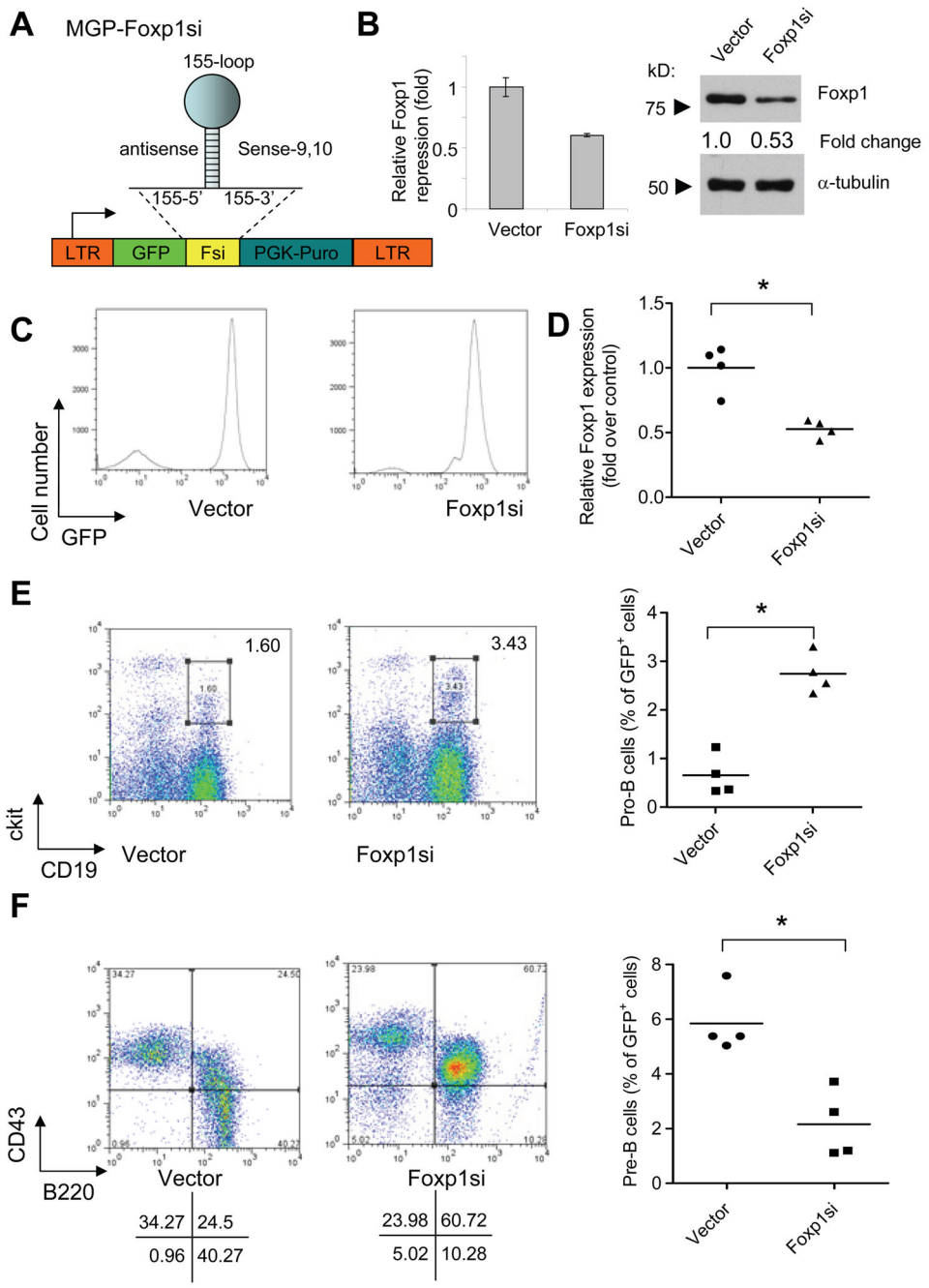

Figure 4. Knockdown of Foxp1 recapitulates miR-34a-induced B-lineage abnormalities

A. Schematic diagram showing the MGP-based construct used to express the Foxp1 siRNA.

B. Left hand panel shows *Foxp1* RNA, measured by RT-qPCR, in 70Z/3 cells infected with either empty vector (Vector) or MGP-Foxp1si (Foxp1si). Right hand panel shows immunoblot analysis of Foxp1 in these cells. The numbers represent the fold expression of Foxp1 at the protein level compared to vector control.

C. GFP expression in the bone marrow of mice (vector and Foxp1si) 2 months after transplant, measured by flow cytometry.

D. *Foxp1* expression in the bone marrow of mice (vector and Foxp1si), as measured by RT-qPCR. Individual dots represent Foxp1 RNA amounts in individual mice, while the bars

show the mean amount for a representative experiment (n=4 for each group; T-test, p=0.0026). Experiments were repeated three times, with similar trends in all three experiments.

E. Analysis of pro-B cells. Left hand panels show representative histograms of the $GFP^{+}IgM^{-}$ negative compartment in control (vector) and Foxp1si mice. The right hand panel shows pro-B cells as a percentage of total GFP+ cells for a representative experiment, with individual mice represented by individual dots and the bars indicating the mean (n=4 per group; T-test, p=0.0004). Three independent experiments showed similar trends.

F. Analysis of pre-B cells. Left hand panels show representative histograms of the GFP+ IgM− compartment in control and Foxp1si mice, below which the percentage of cells in each of the four quadrants is shown. The right hand panel shows pre-B cells as a percentage of total GFP+ cells for a representative experiment, with individual mice represented by individual dots and the bars indicating the mean (n=4 per group; T-test, p=0.005). Three independent experiments showed similar trends.

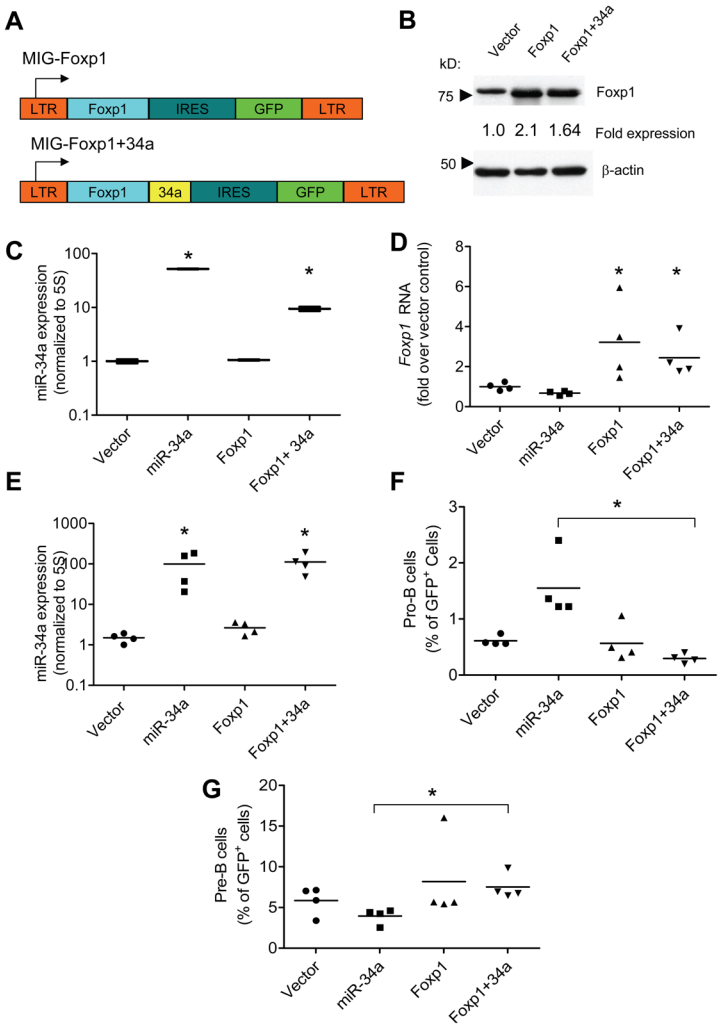

Figure 5. Foxp1 expression rescues the miR-34a induced B cell developmental abnormality

A. Schematic representation of the constructs used to rescue miR-34a-mediated block in B cell development.

B. Immunoblot analysis of extracts from 70Z/3 cells infected with retroviruses depicted in A. The numbers represent relative expression of Foxp1, compared with control.

C. Expression of miR-34a as assayed by RT-qPCR in 70Z/3 cells infected with retroviruses [vector control only, MGP-34a (miR-34a), MIG-Foxp1 (Foxp1), or MIG-Foxp1+34a (Foxp1+34a)]. Individual dots represent measurements in individual mice, and the bars indicate the means for each group (n=4 per group; two independent experiments were performed). Statistically significant differences were found in the expression of miR-34a for the following comparisons: vector vs. miR-34a (T-test, p=0.0001) and vector vs. Foxp1+miR-34a (T-test, p=0.0049).

D. Expression of *Foxp1* in bone marrow, as assayed by RT-qPCR, in mice receiving bone marrow transduced with the same constructs as in C, represented as fold-overexpression over control and normalized to L32. Individual dots represent measurements in individual mice, and the bars indicate the means for each group (n=4 per group; two independent experiments were performed). Statistically significant differences were found in the expression of Foxp1 for the following comparisons: vector vs. Foxp1 (T-test, p=0.036) and vector vs. Foxp1+miR-34a (T-test, p=0.015).

E. Expression of miR-34a in bone marrow, as assayed by RT-qPCR, in mice receiving bone marrow transduced with the same constructs as in C, shown as fold-overexpression over control and normalized to L32. Individual dots represent measurements in individual mice, and the bars indicate the means for each group (n=4 per group; two independent experiments were performed). Statistically significant differences were found in the expression of miR-34a for the following comparisons: vector vs. miR-34a (T-test, p=0.03) and vector vs. Foxp1+miR-34a (T-test, p=0.0056).

F. Enumeration of pro-B cells (CD19+IgM-c-kit+) as a percentage of total GFP+ cells for a representative experiment (n=4 per group; T-test, p=0.0048). Individual dots represent measurements in individual mice, and the bars indicate the means for each group. Two independent experiments were performed.

G. Enumeration of pre-B cells (B220+CD43−IgM−) as a percentage of total GFP+ cells for a representative experiment (n=4 per group; T-test, p=0.0084). Individual dots represent measurements in individual mice, and the bars indicate the means for each group. Two independent experiments were performed.

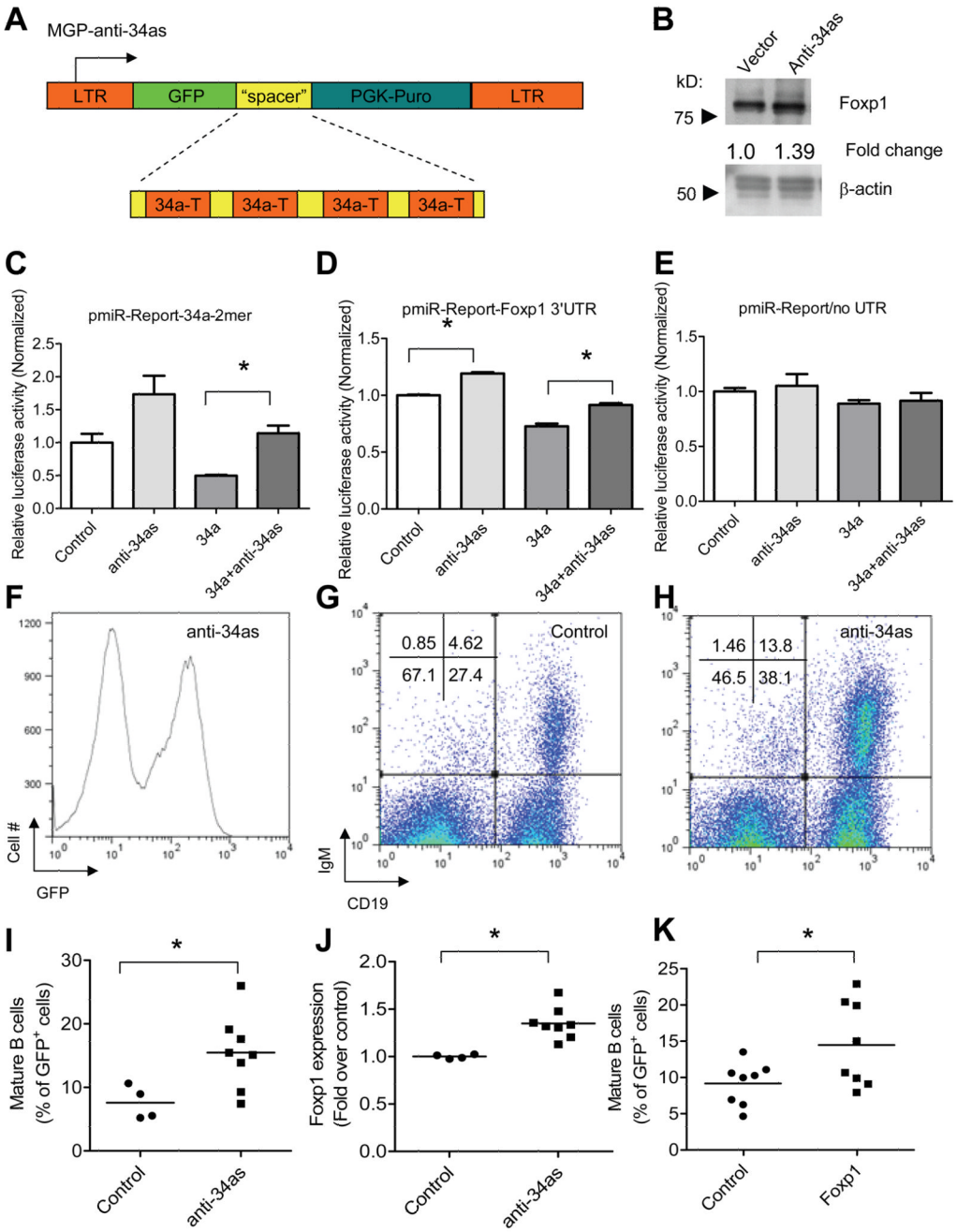

Figure 6. Knockdown of miR-34a using a "sponge" strategy is effective and results in increased mature B cells in the bone marrow

A. Schematic representation of the construct used to knockdown miR-34a expression. The backbone is the MGP vector described previously with the insertion of "spacer miR-Target sites" downstream of the GFP. Abbreviation, 34a-T: miR-34a synthetic target site.

B. Immunoblot analysis of extracts from 70Z/3 cells infected with retroviruses prepared from construct depicted in A. The numbers represent relative expression of Foxp1, compared with control.

C–E. Luciferase assays demonstrate that the knockdown of miR-34a by the construct designated in A is specific for miR-34a target-containing 3′UTRs, graphed as described for Fig 3B. Statistically significant differences were found in relative luciferase activity for the

following comparisons: 34a versus 34a+anti-34as (Fig 6C, T-test, p=0.0053); control vs. anti-34as (Fig 6D; T-test, p=0.0001) and 34a vs. 34a+anti-34as (Fig 6D; T-test, p=0.0033).
F. Bone marrow flow cytometry plot showing that transduction results in the expression of GFP.
G–H. Bone marrow flow cytometry plot showing GFP+ cells plotted for expression of CD19 and IgM. Bone marrow is from a mouse transduced with MGP (Control; G), and a mouse transduced with MGP-anti-34as (H).
I. Enumeration of mature B cells (CD19+IgM+) as a percentage of total GFP+ cells in mice receiving either control or the knockdown construct for miR-34a (n=4 for control MGP; n=8 for anti-34as; T-test, p=0.0285). Individual dots represent measurements in individual mice, and the bars indicate the means for each group. Two independent experiments were performed.
J. Foxp1 expression in bone marrow transductant mice reciveing marrow with either MGP (Control) or anti-34as marrow (n=4 for control MGP; n=8 for anti-34as; T-test, p=0.0022). Individual dots represent measurements in individual mice, and the bars indicate the means for each group. Two independent experiments were performed.
K. Enumeration of mature B cells (CD19+IgM+) as a percentage of total GFP+ cells in mice recieivng either control or constitutive expression contruct for Foxp1 (n=8 for control; n=8 for MIG/Foxp1; T-test, p=0.0383). Individual dots represent measurements in individual mice, and the bars indicate the means for each group. Two independent experiments were performed.